

# **Main study - Simulation of copper lid manufacturing**

Paul Åkerström  
Swerea MEFOS

October, 2013

## Abstract

In the current work numerical simulations of selected steps of the manufacturing of copper lids for use as part of copper canisters for spent nuclear fuel have been treated. The main aim has been to study the final location and shape of initial postulated defects/damages on the barrel, top and bottom surfaces of the work-piece by numerical FE-simulations. Further, based on the machining of the manufactured lid to its final dimensions, judgments are made regarding how much of the postulated defects/damages that will remain. All numerical FE-simulations have been conducted using the commercial software LS-Dyna 971 using 2D-axisymmetric models. Two types of surface originating cracks, 25 small internal particles spread in the initial work-piece for tracing and one type of barrel surface damage have been treated. For the postulated cracks studied in the case of lid manufacturing, it has been shown that the half-elliptical crack in the lowest position and the two lower circular cracks tend to enter the material of the lid that remains after machining to final dimensions. The handling damage does not enter the material that remains after machining. The postulated particles were used to illustrate the material flow during the specified manufacturing steps. It has been shown that 10 out of 25 postulated particles end up within the material of the finished machined lid. None of the particles initially located on the workpiece barrel surface, top or bottom surfaces will be present in the machined lid.

# Content

<b>1</b>	<b>Introduction</b>	<b>4</b>
1.1	Initial defects and damages	5
<b>2</b>	<b>FE-model descriptions</b>	<b>8</b>
2.1	Elements and contacts	8
2.2	Friction	8
2.3	Constitutive models	8
2.4	Lower tool	9
2.5	Defects	9
<b>3</b>	<b>Simulations and results</b>	<b>10</b>
3.1	Half elliptical cracks	11
3.2	Handling damages	14
3.3	Circular cracks	17
3.4	Postulated particles	19
<b>4</b>	<b>Discussion and conclusions</b>	<b>26</b>
	<b>References</b>	<b>27</b>

# 1 Introduction

In this work, numerical simulations of selected steps of the manufacturing of copper lids as part of copper canisters for spent nuclear fuel have been treated. The main aim has been to study the movement and shape of postulated damages/defects, as illustrated in section 1.1, during the manufacturing of the lid and to estimate the size of initial damages/defects that will be completely removed during the final machining. This is to find and suggest improvements to parts of the manufacturing process and/or tool designs to have sufficient high margins to completely remove the defects and damages during the final machining. The method used for the manufacturing of the lids comprises a number of steps that briefly are described below. A more comprehensive description can be found in “Tillverkning av kapselkomponenter” (SKBdoc 1175208).

1. Furnace heating to  $\sim 780$  °C of an initial cylindrical workpiece with a diameter and height of 500 and 739 mm (cold dimensions), respectively. The billet mass is 1,300 kg.
2. Upsetting of billet, where the billet is reduced by 290 mm from its initial hot height, 749 mm, to 459 mm while pressing it between two planar tool parts, see Figure 1-1.
3. Pressing a tool according to Figure 1-2 and Figure 1-3 into the workpiece by 190 mm.
4. Closed die forging by using a flat upper tool. In this step the workpiece is pressed into the cavity of the lower tool. The force available in the hydraulic press used is limited to 4,500 tons, which is insufficient to completely fill the workpiece into the cavity of the lower tool (not giving the workpiece its final form).
5. Cogging of the workpiece with the upper tool illustrated in Figure 1-4.
6. After cooling to room temperature, the workpiece is machined to its final dimensions.



**Figure 1-1.** *Upsetting of the workpiece in the reference process.*

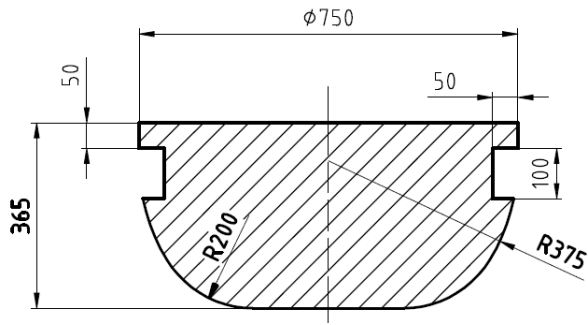


*Figure 1-2. Tool used in the step before closed die forging.*



*Figure 1-3. The state where the upper tool is pressed 190 mm into the workpiece.*



*Figure 1-4. Cogging with tools and workpiece shown.*

In this work, the steps 2-4 in the reference method have been simulated to study the movement and shape of the postulated defects and damages. In a previous work, “Simulation of forging of lids with different upper tools” (SKBdoc 1392448), studies of plastic strain distribution in the work-piece during selected steps of the manufacturing process have been treated. The ingot that is heated to 780 °C in the furnace in step 1 is estimated from measurements to have an average temperature of 750 °C when the actual pressing begins.

## 1.1 Initial defects and damages

In this section the different postulated defects and handling damages are illustrated. Figure 1-5 to Figure 1-8 illustrates the initial locations and sizes of the defects and damages treated in this work.

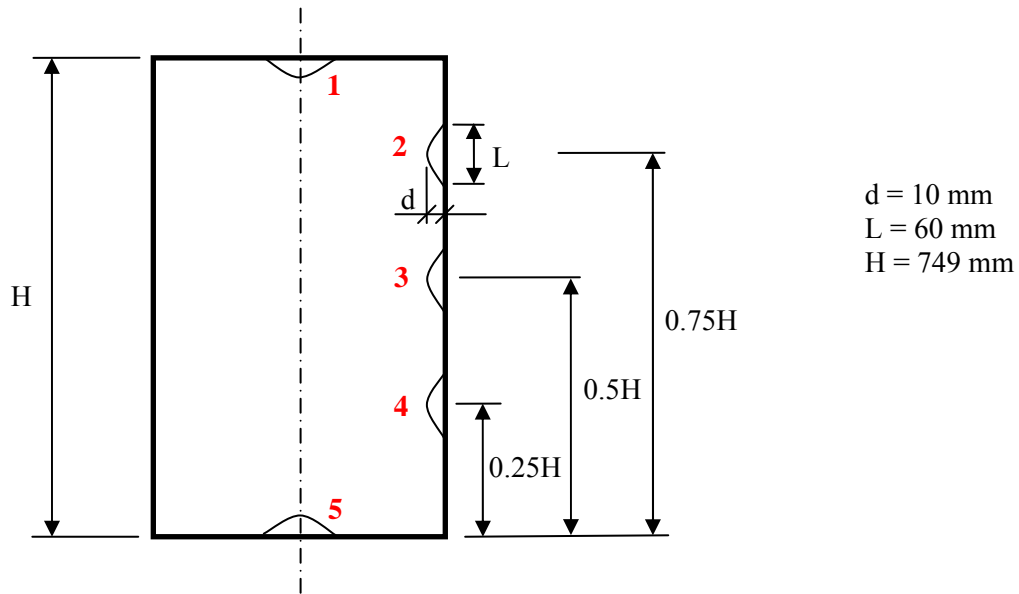


**Figure 1-5.** Surface originating half-elliptical cracks on the barrel surface and at the center of the top and bottom surfaces.

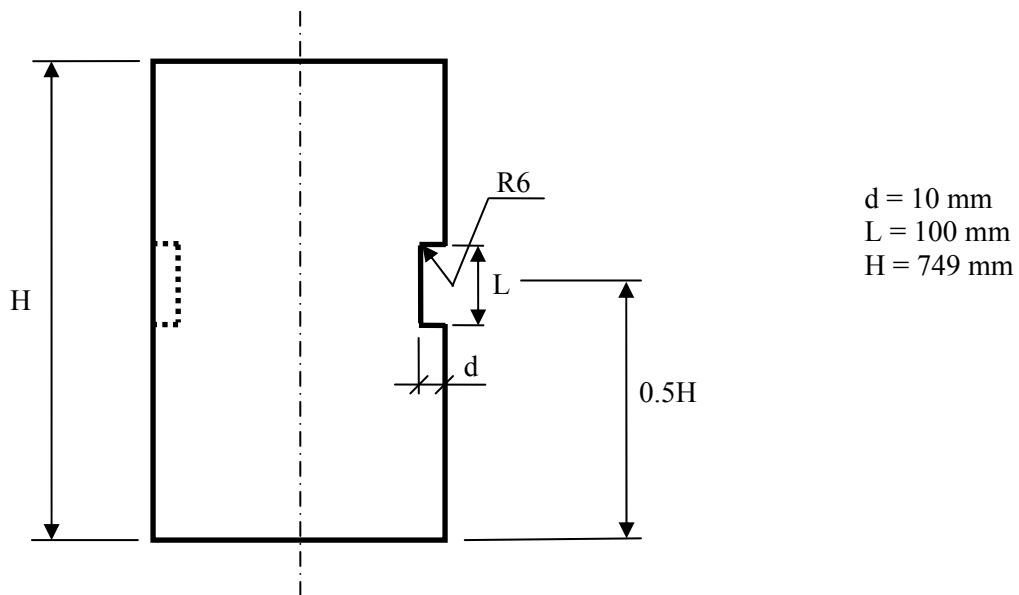


**Figure 1-6.** Handling damage on the barrel surface of the workpiece. Note that this type of damage will correspond to a circumferential groove in the 2D axi-symmetrical case as employed here.

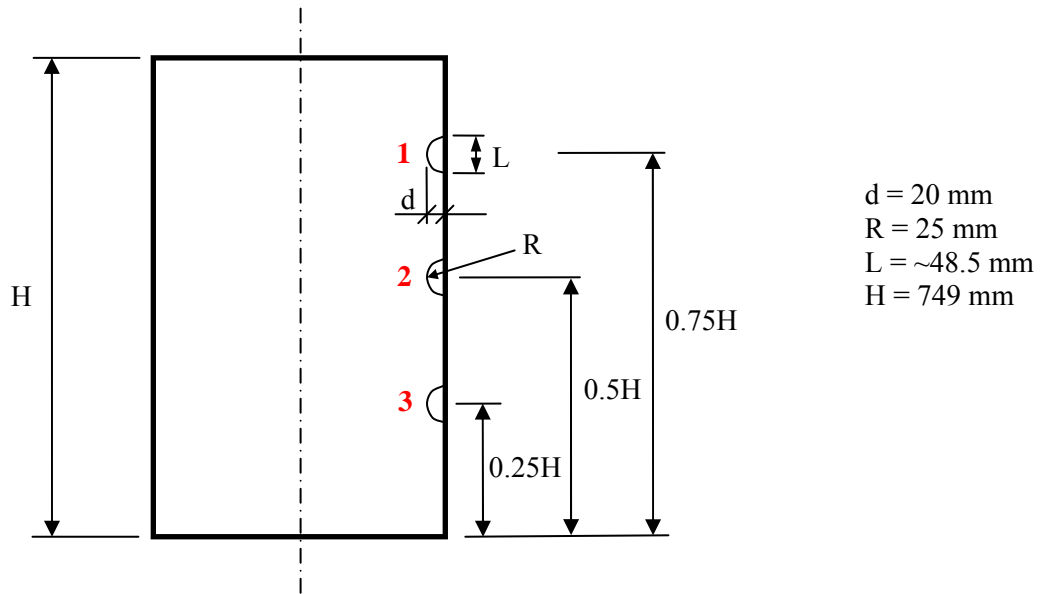


**Figure 1-7.** Surface originating circular cracks on the barrel surface.

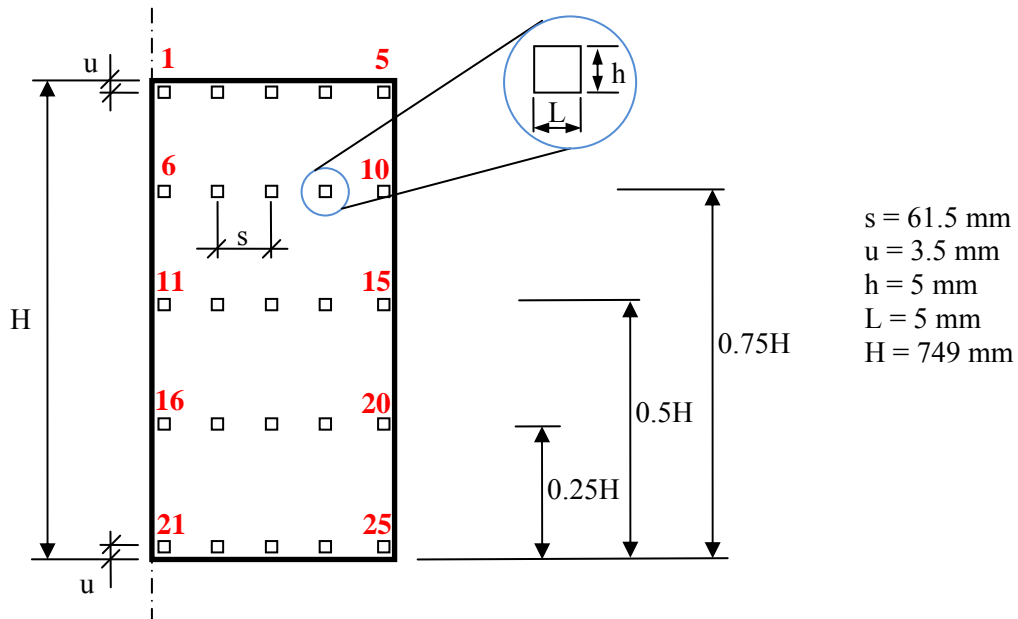


**Figure 1-8.** Internal “defects” modeled initially as squares of 5 x 5 mm, note the location of the symmetry (center) line. The number of “tracing squares” is 25, whereas the numbering starts at the upper left corner and finish in the lower right corner of the workpiece.

## 2 FE-model descriptions

The FE-simulations performed have been conducted using the commercial software system LS-DYNA 971R6 (Hallquist 2006). All simulations have been performed thermo-mechanically coupled. In LS-Dyna, the coupling is performed using a staggered approach, meaning that the thermal step precedes the mechanical steps and the thermal field is calculated based on the previous (converged) mechanical configuration. All LS-DYNA simulations have been performed using an explicit time integration scheme and a fully implicit (iterative) thermal solution procedure. All cases studied have been modeled as 2D-axisymmetric, meaning that the problem is assumed not to have any variations in the circumferential direction. This means that any variations in either temperature or friction in that direction cannot be modeled and simulated. Further, effects on the workpiece behavior (plastic flow, shape etc.) due to variations in tool shape or initial workpiece geometry along the circumference direction cannot be studied. The angular dimension of the axisymmetric model used is one radian and in order to obtain the total forming force a multiplication of  $2\pi$  radians is necessary.

### 2.1 Elements and contacts

The element variant used in LS-DYNA in the case of 2D-axisymmetric simulations is the Type 15 volume weighted axisymmetric Galerkin element for both the rigid tool parts and the workpiece. In LS-DYNA, penalty based contacts have been employed and the contact is an automatic variant called

\*CONTACT\_2D\_AUTOMATIC\_SURFACE\_TO\_SURFACE\_THERMAL, in which the thermal heat transfer across the contact interface is used. The thermal contact is set to be active if the distance between the contacting instances not are greater than 0.1 mm and the heat transfer is regarded not to be pressure dependent, as in “Process simulation of large copper tube extrusions” (SKBdoc 1351636). The heat transfer conductance used has been adapted from the same work.

### 2.2 Friction

The friction model used for the contacts is of Coulomb type. In the current work the static and dynamic coefficients of friction have been set equal to 0.2 meaning that the frictional coefficient is regarded as constant independent of the relative sliding velocity. In order to limit the maximum shear stress (force) in the contacts from reaching unrealistic levels, a constant upper limit value of 6 MPa has been chosen based on work “Main study - Copper tube extrusion” (SKBdoc 1377246) for lubricated contacts.

### 2.3 Constitutive models

The mechanical constitutive law used in LS-DYNA is an elastic-viscoplastic model with strain rate and temperature dependent hardening curves for the workpiece material. The workpiece hardening data (stress versus strain data) used is taken from “Control and effects of grain size in extruded copper” (SKBdoc 1265008). During the different deformation processes, 90 percent of the plastic work is assumed to be converted into heat.

All tool steel parts are modeled as rigid, and the thermal data corresponds to tool steel material 34CrNiMo6. The thermal material model used (both for tools and work-piece) is an isotropic thermal model with temperature dependent thermal conductivity and specific heat.



## 2.4 Lower tool

The lower tool model is based on the tool geometry of the production tool which is used in 2013. Using the calculated volume of the cavity in the lower tool together with a mass density of  $8960 \text{ kg/m}^3$  (for copper at room temperature) gives a theoretical workpiece mass close to 1250 kg, meaning that the used workpiece has an extra mass of 50 kg or 4 %. The height,  $h$  of the excess hot material as defined in Figure 2-1, assuming that no flash is formed and the tool cavity is fully filled, can be estimated to 7.1 mm.

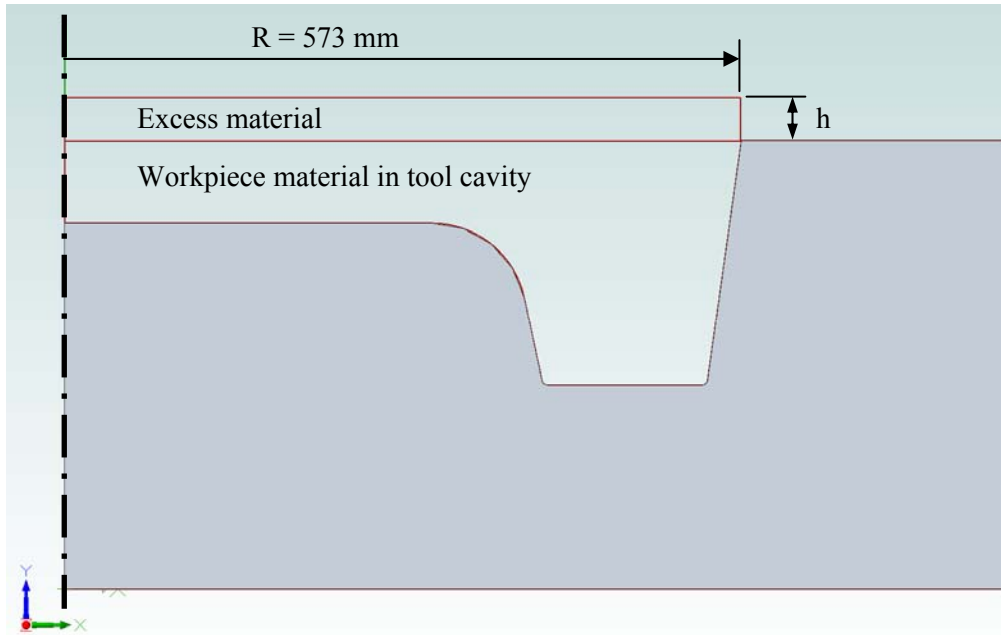


**Figure 2-1.** Definition of the excess material and its height. A workpiece mass of 1,300 kg gives a theoretical excess height,  $h$ , close to 7.1 mm.

## 2.5 Defects

The cracks and internal defects have been modeled by using elements with “null material” tied by contact to the underlying 2D-axisymmetric mesh. This means that the material flow is unaffected by the addition of these elements. It should be noted that it is here assumed that the actual defects does not influence the overall flow behavior of the copper material and thereby makes this approach possible.

### 3 Simulations and results

In this section the simulations performed using the reference production method; steps 2-4 described in the introduction section will be presented. The location and size of the initially defined defects/damages according to section 1.1 will be given for production steps 2-4. In the FE-simulations, step 5 above is not simulated, instead step 4, closed die forging is applied until the work-piece has filled the cavity of the lower tool. This procedure is not possible in the current process because it will need a press force that exceeds the capacity of the equipment. The real cogging process is not well defined and contains more than 50 strokes. It will not be reasonable to try to simulate the process with all the uncertainties found in the process description. The 2D-axisymmetric case is here selected and the chosen simplifications is judged to give a good estimate of the material flow inside the tool cavity but the material flow of the workpiece top will not be correct. In all the simulations performed, a press speed of 70 mm/s (for the upper tool) has been used, which is taken from Ssemakula (2004). For more information regarding the effective plastic strain distributions and forming forces during step 2 and 3, the reader is referred to “Simulation of forging of lids with different upper tools” (SKBdoc 1392448). Some of the Figures shown in the following illustrate the position of the postulated defects and cracks in relation to the finished machined lid. The position of the final machined geometry is determined by the actual machining strategy and is here set to be centered in y-direction in the cavity of the lower tool, according to Figure 3-1. Typical forming forces for the manufacturing steps 2-4 are shown in Figure 3-2. Note the high calculated force developing, close to 30,000 ton, during step 4 when the workpiece fills the cavity of the lower tool and flash is formed. The available force in the press is limited to 4,500 tonnes.

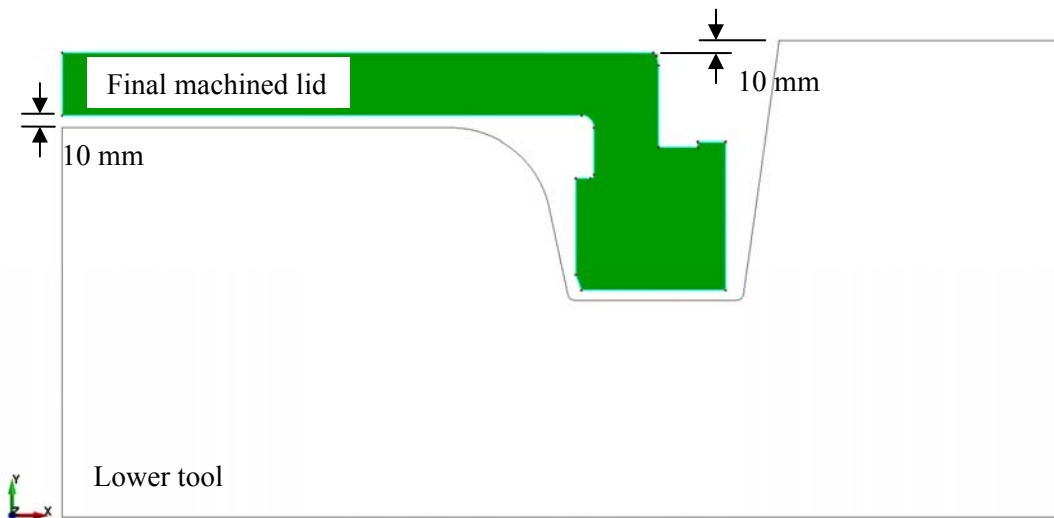


**Figure 3-1.** Assumed position of the machined lid in relation to the lower tool.

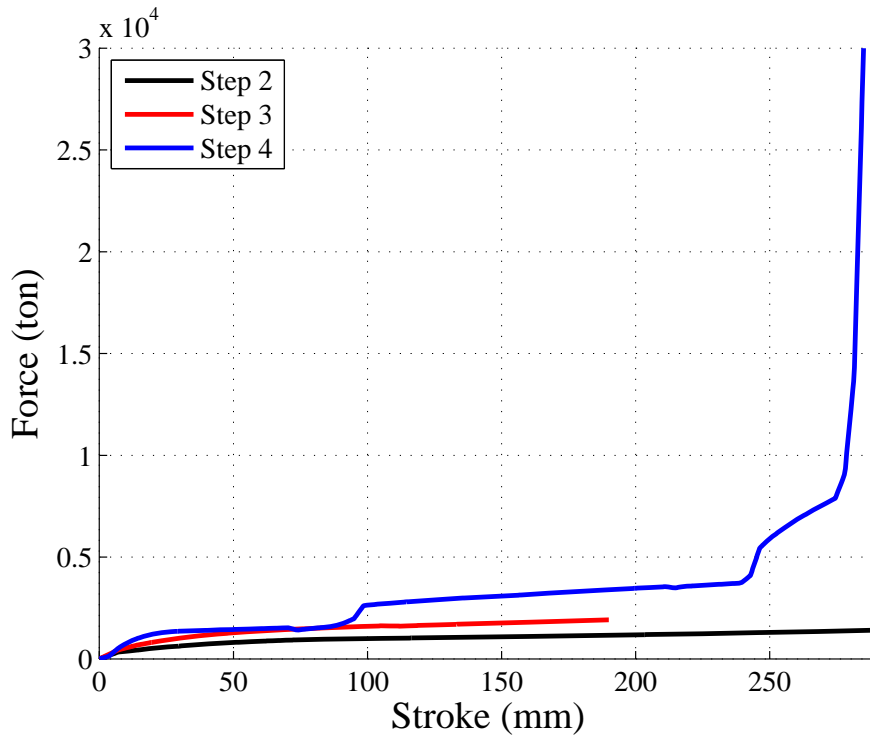


*Figure 3-2. Calculated forming forces for lid manufacturing steps 2-4.*

### 3.1 Half elliptical cracks

Half elliptical cracks as illustrated in Figure 1-5 have been used for the first variant. In Figure 3-3 to Figure 3-7, the locations of the cracks after each step during the manufacturing are shown in red. The geometry of the final machined lid is shown in green. The sizes of the individual cracks after each manufacturing step are given in Table 3-1. It can be noticed in Figure 3-6 and Figure 3-7 that the cracks initially located on the barrel surface are ending up at slightly different positions after step 4 depending on the effective plastic strains and stresses are inherited from the second step or not. It can be seen in Figure 3-6 and Figure 3-7 that the lowest crack (no 4) on the barrel surface ends up partially inside the green marked area (~3 mm).

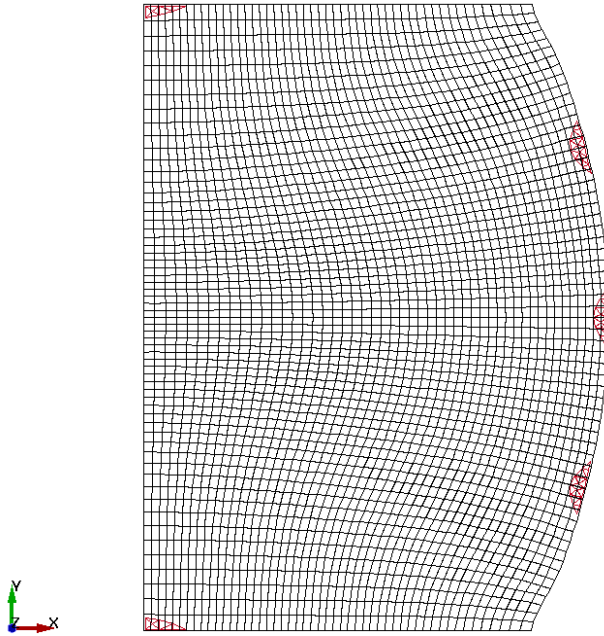


**Figure 3-3.** Location of cracks in workpiece after upsetting, step 2.

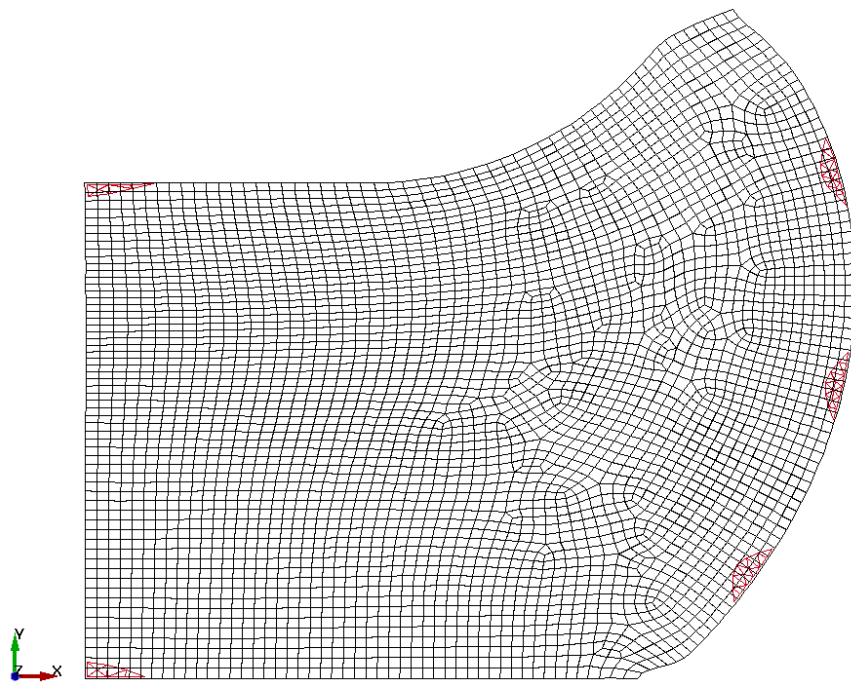


**Figure 3-4.** Location of cracks in workpiece after piercing, step 3, with inherited stresses and effective plastic strains from step 2.

Cracks on the mid and lower part of the barrel surface are more critical than cracks on the upper part. Cracks which are originating from the mid and lower part will end up close to the corners of the lid flange. These positions are the most critical because of the low machining allowance.

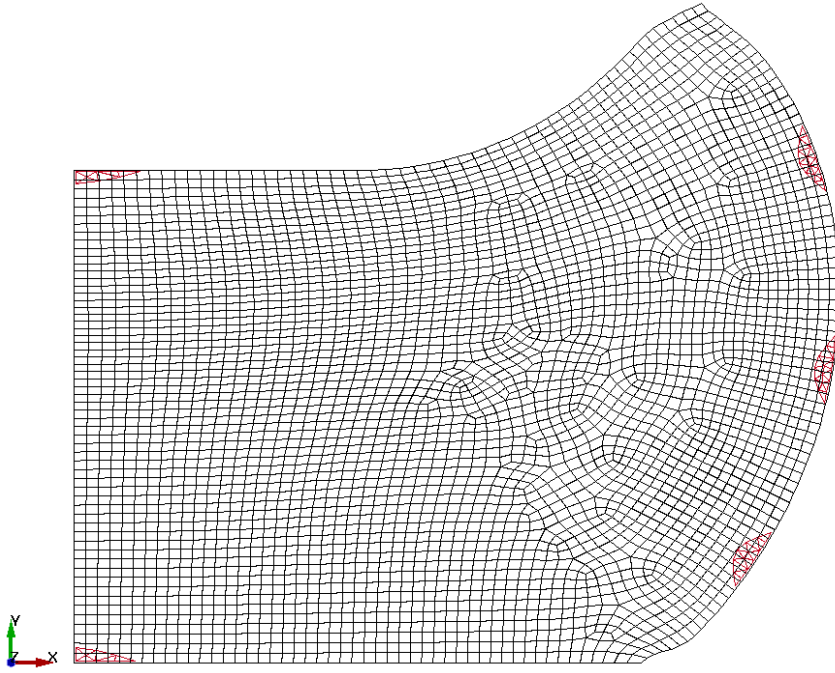


**Figure 3-5.** Location of cracks in workpiece after piercing, step 3, without inherited stresses and effective plastic strains from step 2.

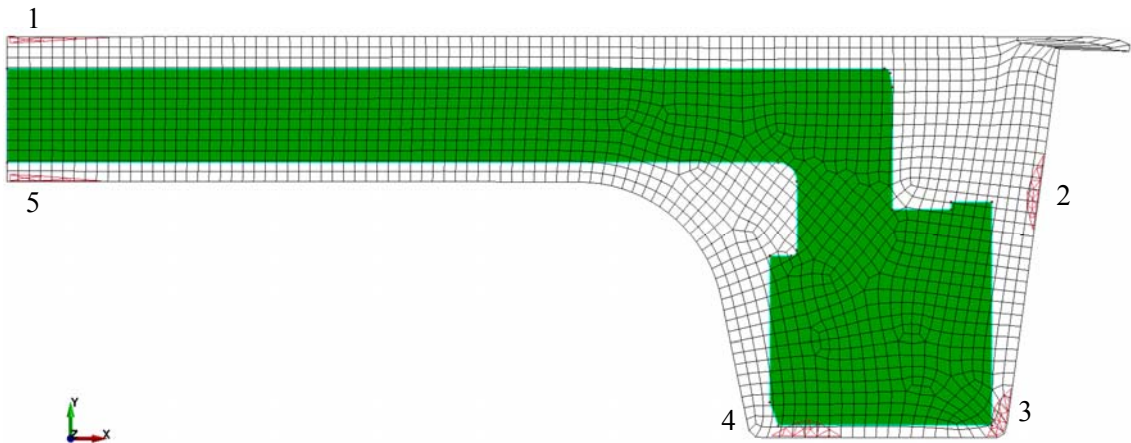


**Figure 3-6.** Location of cracks in workpiece after the closed die forging, step 4, with inherited stresses and effective plastic strains from step 2 and 3. Note that the workpiece is at room temperature.

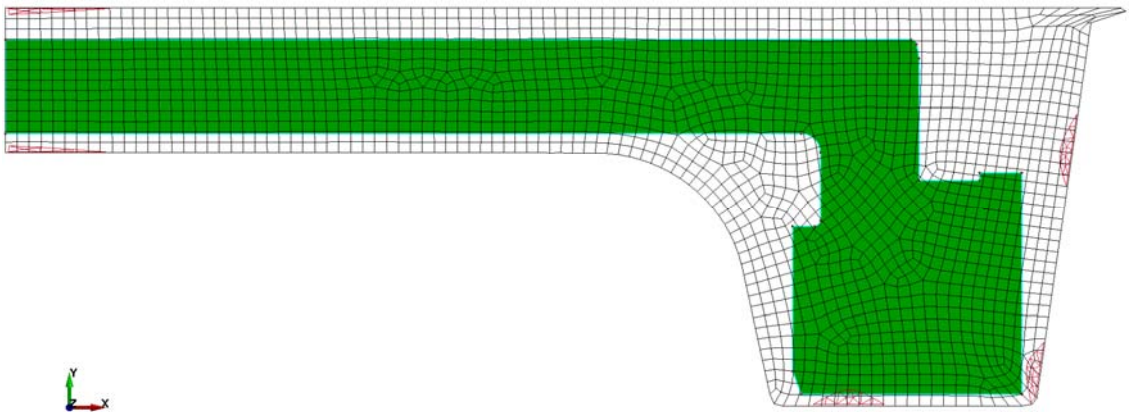


**Figure 3-7.** Location of cracks in workpiece after the closed die forging, step 4, with inherited stresses and effective plastic strains from step 3. Note that the workpiece is at room temperature.

**Table 3-1. Crack sizes after the different manufacturing steps for the half-elliptical variant. The value given within parenthesis is for the workpiece without inherited effective plastic strains from the upsetting operation.**

Step / crack no.	Initial dimensions		Final dimensions	
	d (mm)	L (mm)	d (mm)	L (mm)
Upsetting / 1	10	60	8.5	60
Upsetting / 2	10	60	10.5	40
Upsetting / 3	10	60	10	41
Upsetting / 4	10	60	10.5	40
Upsetting / 5	10	60	8.5	60
Piercing / 1	8.5	60	6 (6.5)	72 (70)
Piercing / 2	10.5	40	9 (9)	76 (76)
Piercing / 3	10	41	9 (9)	74 (74)
Piercing / 4	10.5	40	11 (11)	72 (70)
Piercing / 5	8.5	60	8 (7.5)	62 (64)
Closed die forging / 1	6 (6.5)	72 (70)	3 (3)	112 (108)
Closed die forging / 2	9 (9)	76 (76)	6 (6)	41 (39)
Closed die forging / 3	9 (9)	74 (74)	8 (7)	29 (33)
Closed die forging / 4	11 (11)	72 (70)	8.5 (8)	37 (38)
Closed die forging / 5	8 (7.5)	62 (64)	3 (3)	100 (102)

### 3.2 Handling damages

A handling damage as illustrated in Figure 1-6 has been used for the second variant of surface defect. In Figure 3-8 to Figure 3-12, the locations of the damage after each step during the manufacturing are shown. The geometry of the final machined lid is shown in green. The damage sizes, according to definitions in Figure 1-6 is given in Table 3-2 for each manufacturing step. The postulated handling damage ends up in the vicinity of the “lower right corner” of the tool which can be seen in Figure 3-11 and Figure 3-12. The final depth, 3.5 mm, for the handling damage must be regarded to be approximate due to the known fact that remeshing algorithms tend to change small complex boundaries each remeshing cycle. Therefore the number of remeshing steps has been kept to a minimum with regard to maintaining “good” element shapes.

Handling damages on the mid and lower part of the barrel surface are more critical than damages on the upper part. Damages on the mid-height seem to end up close to the outside corner of the lid flange. This is the most critical point because of the low machining allowance.

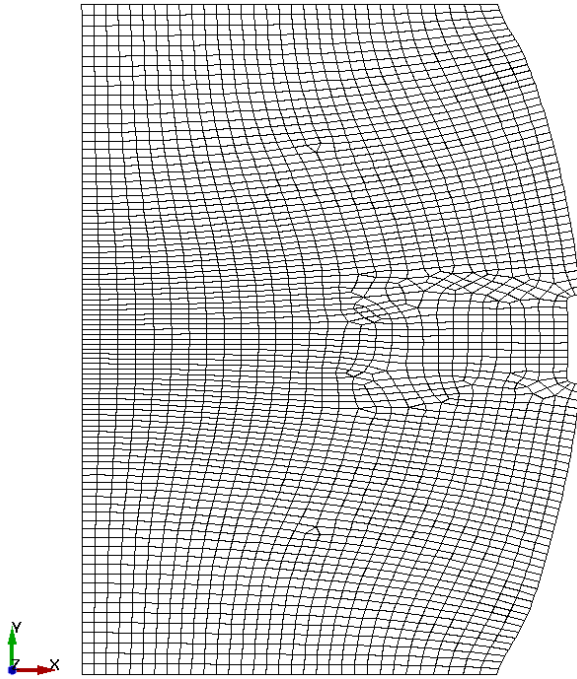


**Figure 3-8.** Location of the barrel surface handling damage of the workpiece after upsetting, step 2.

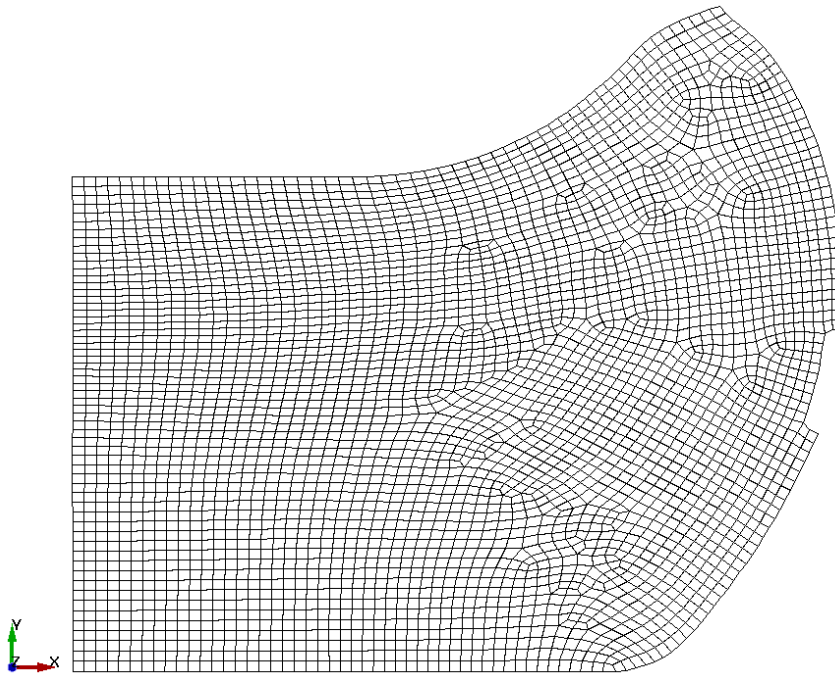


**Figure 3-9.** Location of the handling damage on the barrel surface of the workpiece after piercing, step 3, with inherited stresses and effective plastic strains from step 2.



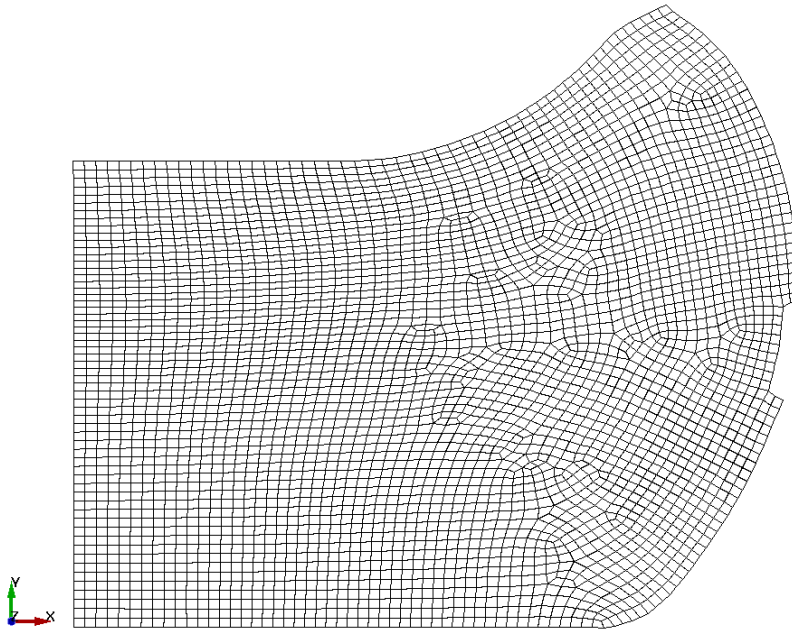


**Figure 3-10.** Location of the handling damage on the barrel surface of the workpiece after piercing, step 3, without inherited stresses and effective plastic strains from step 2.

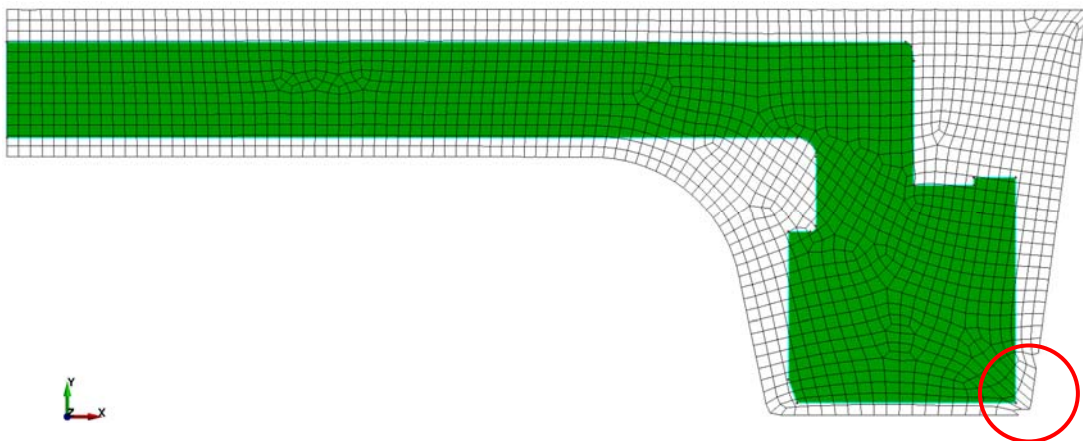


**Figure 3-11.** Location of handling damage in workpiece after the closed die forging, step 4, with inherited stresses and effective plastic strains from step 2 and 3. Note that the workpiece is at room temperature.

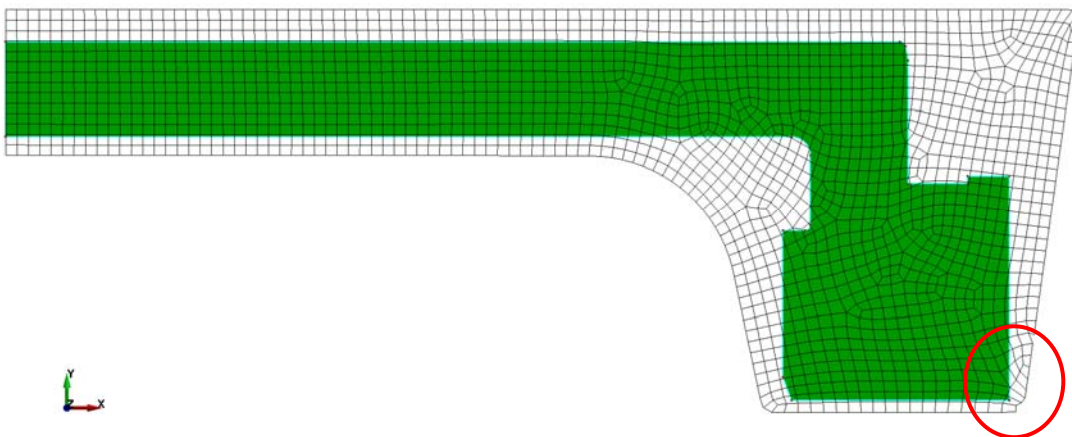


**Figure 3-12.** Location of handling damage in the workpiece after the closed die forging, step 4, with inherited stresses and effective plastic strains from step 3. Note that the workpiece is at room temperature.



**Table 3-2. Damage size after the different manufacturing steps for the postulated handling damage. The value given within parenthesis is for the workpiece without inherited effective plastic strains from the upsetting operation.**

Step	Initial dimensions		Final dimensions	
	d (mm)	L (mm)	d (mm)	L (mm)
Upsetting	10	100	10	62
Piercing	10	62	9.5 (9.5)	58 (57)
Closed die forging	9.5 (9.5)	58 (57)	3.5 (3.5)	35 (43)

### 3.3 Circular cracks

Circular cracks located on the barrel surface as illustrated in Figure 1-7 have been used for the third variant. In Figure 3-13 and Figure 3-17, the locations of the cracks after each step during the manufacturing are shown in red. The geometry of the final machined lid is shown in green. The sizes of the individual cracks after each manufacturing step are given in Table 3-3. It can be noticed visually in Figure 3-16 and Figure 3-17 that the cracks initially located on the barrel surface are ending up at slightly different positions after step 4 depending on the effective plastic strains and stresses are inherited from the second step or not. It can be seen in Figure 3-16 and Figure 3-17 that the two lowest cracks end up partially inside the green marked area. This means that after machining crack 3 will have a remaining depth of 13 mm and crack will have a remaining depth of 8 mm. The position of the final machined geometry is assumed to be centered in y-direction in the cavity of the lower tool, according to Figure 3-1.

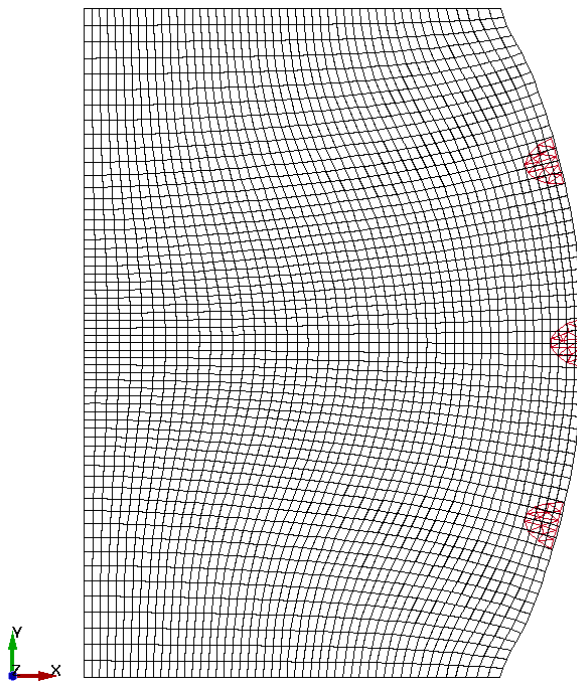


**Figure 3-13. Location of circular cracks in workpiece after upsetting, step 2.**

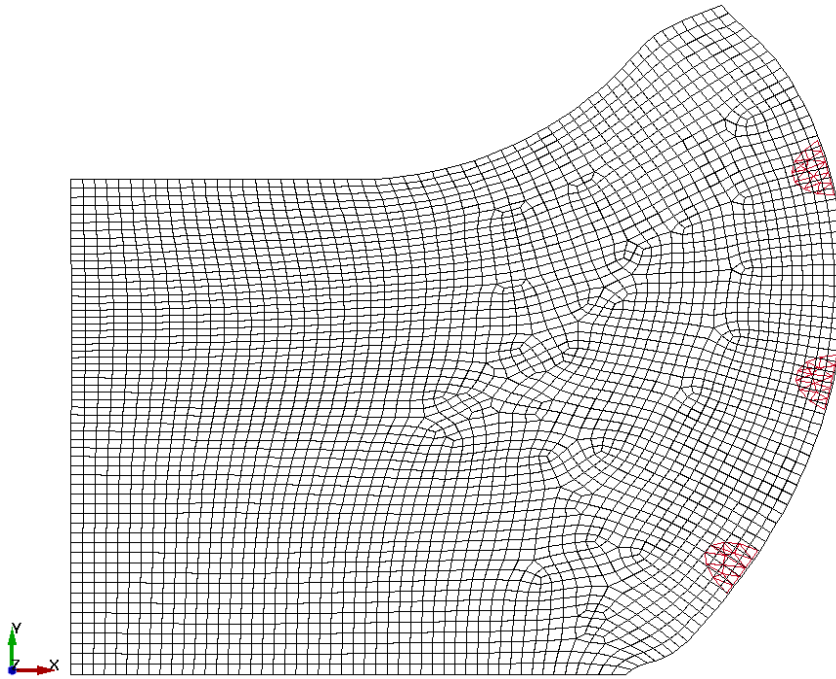


**Figure 3-14.** Location of circular cracks in workpiece after piercing, step 3, with inherited stresses and effective plastic strains from step 2.

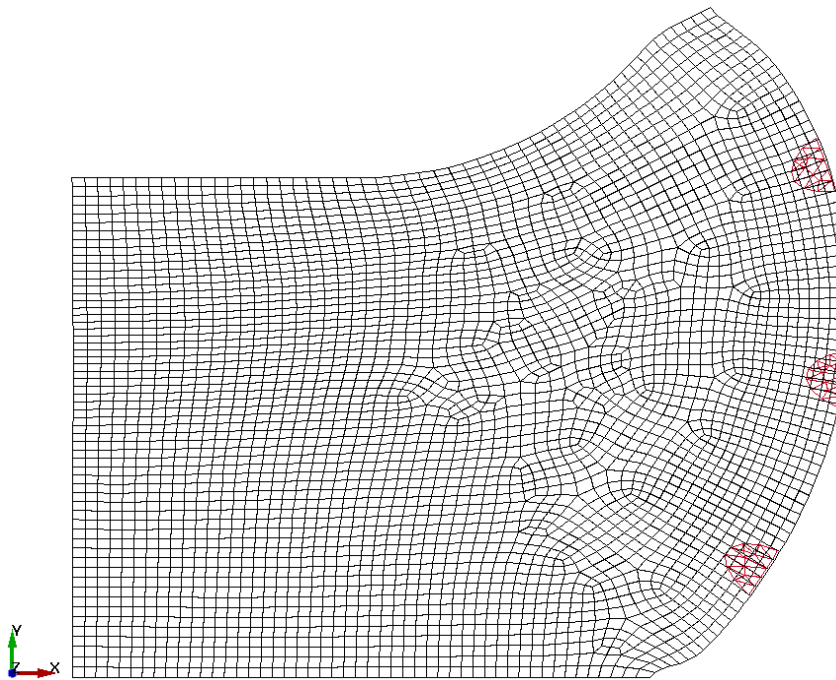


**Figure 3-15.** Location of circular cracks in workpiece after piercing, step 3, without inherited stresses and effective plastic strains from step 2.

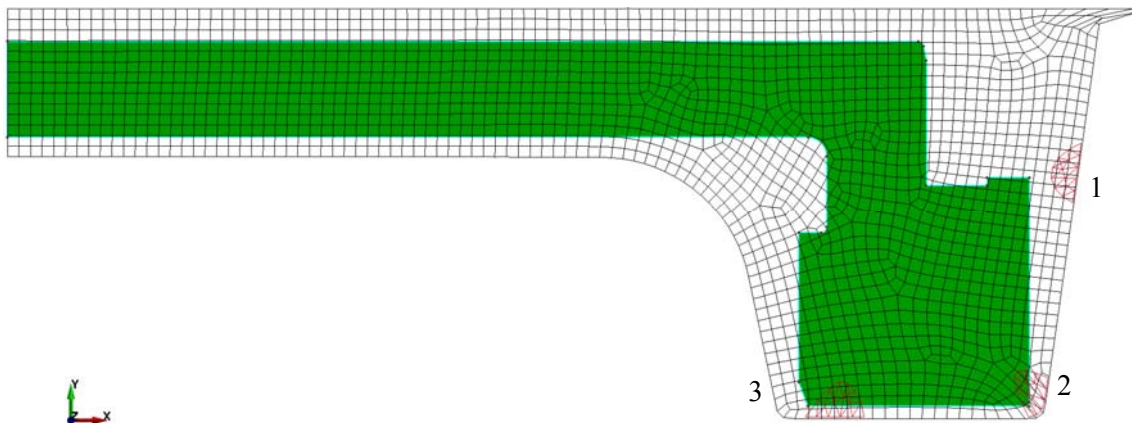


**Figure 3-16.** Location of circular cracks in workpiece after the closed die forging, step 4, with inherited stresses and effective plastic strains from step 2 and 3. Note that the workpiece is at room temperature.

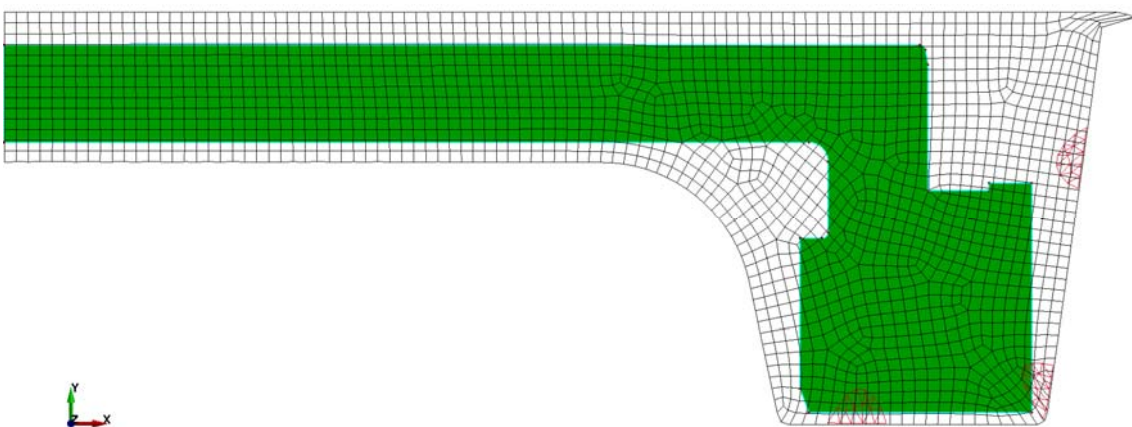


**Figure 3-17.** Location of circular cracks in workpiece after the closed die forging, step 4, with inherited stresses and effective plastic strains from step 3. Note that the workpiece is at room temperature.

**Table 3-3.** Crack sizes after the different manufacturing steps for circular cracks. The value given within parenthesis is for the workpiece without inherited effective plastic strains from the upsetting operation.

Step / crack no.	Initial dimensions		Final dimensions	
	d (mm)	L (mm)	d (mm)	L (mm)
Upsetting / 1	20	48.5	22	32.5
Upsetting / 2	20	48.5	21	33
Upsetting / 3	20	48.5	22	32.5
Piercing / 1	22	32.5	19 (19)	31 (31)
Piercing / 2	21	33	19 (19)	30 (30)
Piercing / 3	22	32.5	22 (22)	29 (28)
Closed die forging / 1	19 (19)	31 (31)	13 (13)	31.5 (32)
Closed die forging / 2	19 (19)	30 (30)	24 (16)	23 (29)
Closed die forging / 3	22 (22)	29 (28)	19 (18)	31 (31)

Cracks on the mid and lower part of the barrel surface are more critical than cracks on the upper part. Cracks which are originating from the mid and lower part will end up close to the corners of the lid flange. These positions are the most critical because of the low machining allowance.

### 3.4 Postulated particles

In this part 25 postulated particles initially located as illustrated in Figure 1-8 have been studied. In Figure 3-18 to Figure 3-22, the locations of the particles after each step during the manufacturing are shown in red. The geometry of the final machined lid is shown in green. The sizes of the individual particles after each manufacturing step are given in Table 3-4. It can be seen in Figure 3-21 and Figure 3-22 that particles number 6, 8, 11, 12, 13, 14, 16, 17, 18 and 19

ends up inside the green marked area. To increase the visibility of the motion of the particles during the closed die forging, step 4, trace lines have been defined to follow a node belonging to each pair of elements defining every particle as illustrated in Figure 3-23. Figure 3-24 to Figure 3-27 shows the tracing of the particles during the manufacturing step 4.

The material flow is mainly compressive in height direction for the central part of the lid. For the outer part of the lid the material flow is dominant for the radial (x) direction. Typically particles number 13 and 14 are moving both in (x) and negative (y) direction as the cavity in the lower tool is filled.

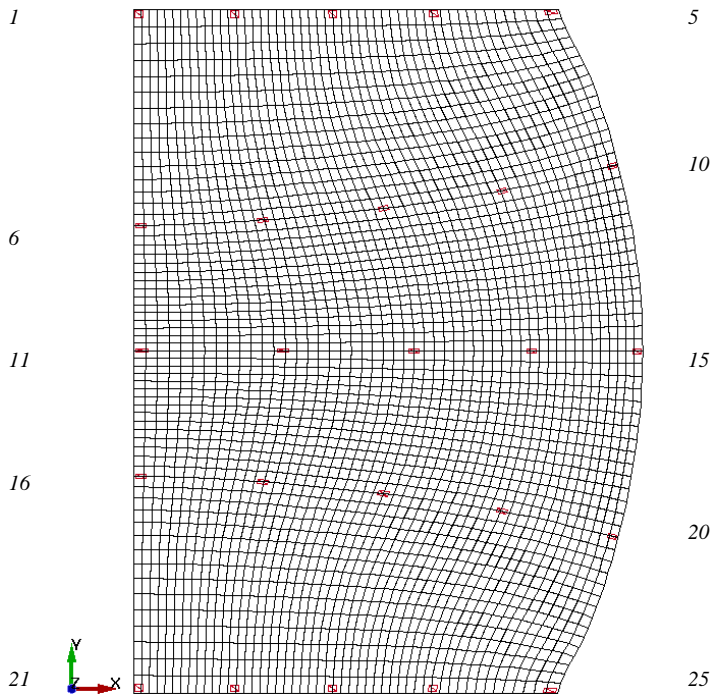


**Figure 3-18.** Location of particles in the workpiece after upsetting, step 2.

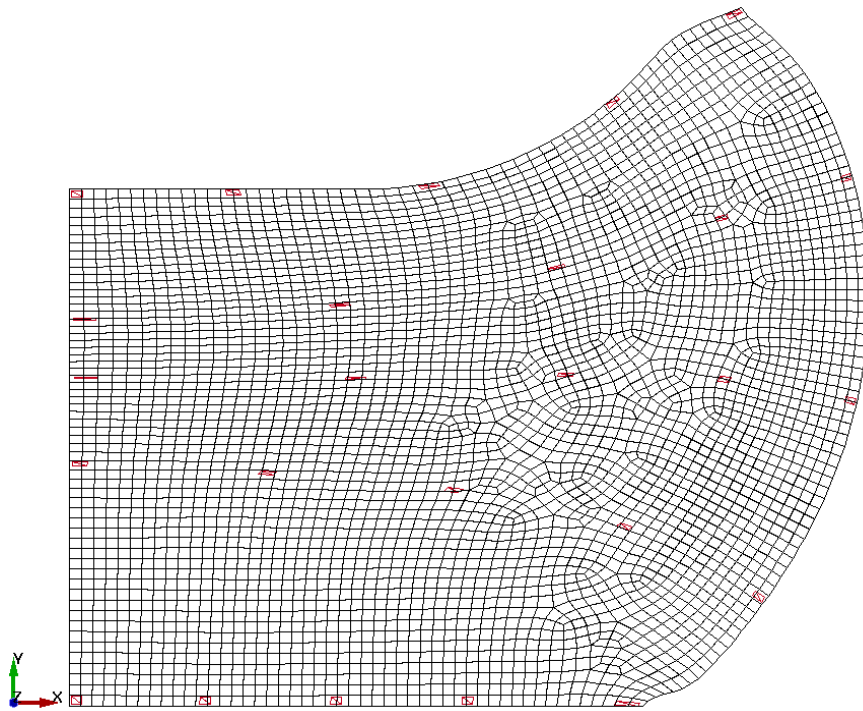


**Figure 3-19.** Location of particles in the workpiece after piercing, step 3, with inherited stresses and effective plastic strains from step 2.

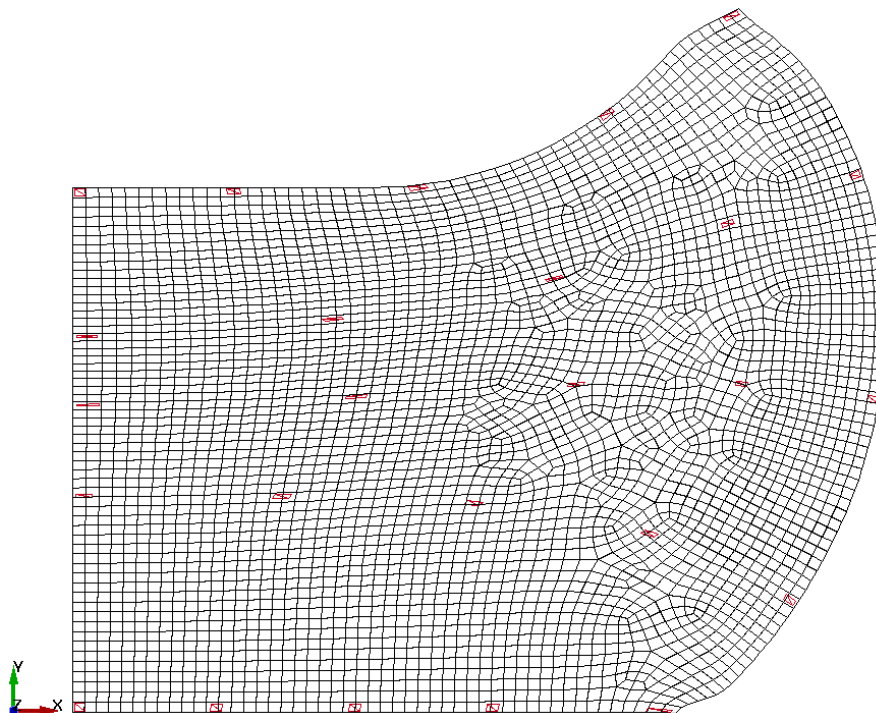


**Figure 3-20.** Location of particles in the workpiece after piercing, step 3, without inherited stresses and effective plastic strains from step 2.



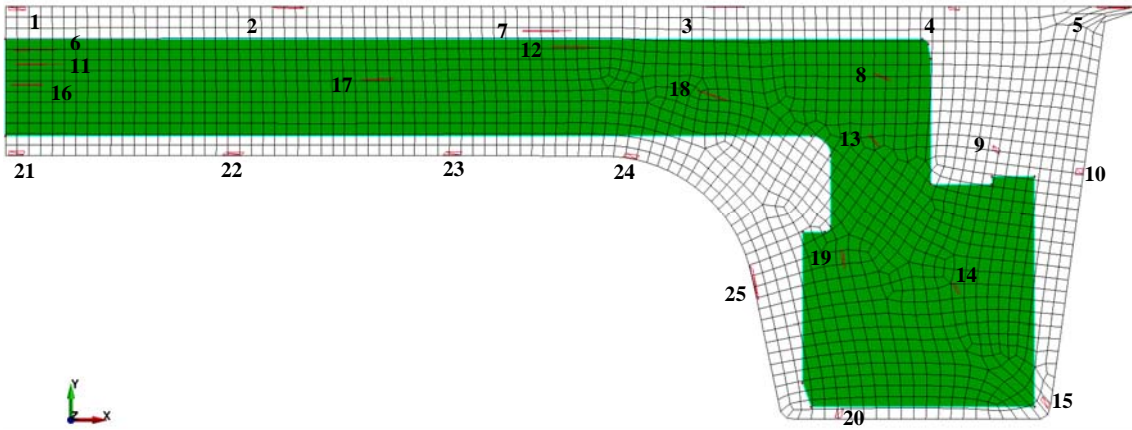


**Figure 3-21.** Location of particles in the workpiece after the closed die forging, step 4, with inherited stresses and effective plastic strains from step 2 and 3. Note that the workpiece is at room temperature.

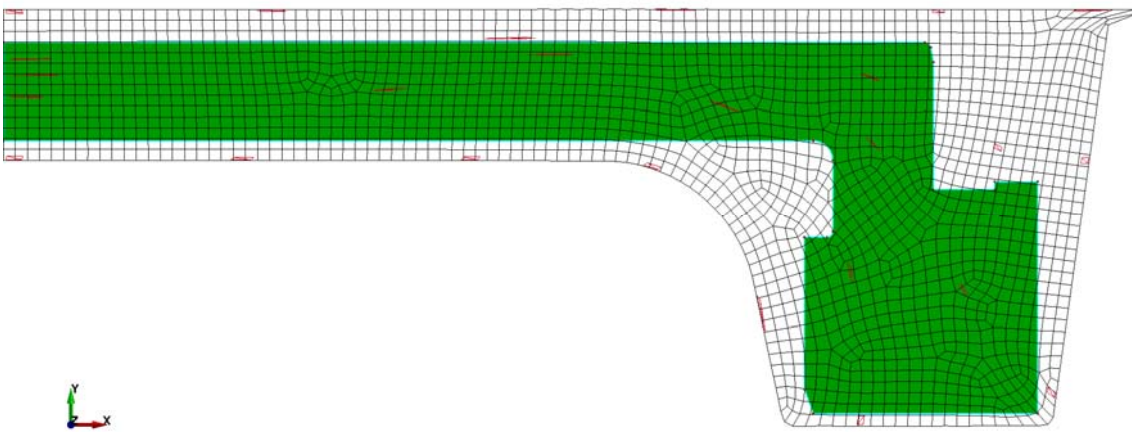


**Figure 3-22.** Location of particles in the workpiece after the closed die forging, step 4, with inherited stresses and effective plastic strains from step 3. Note that the workpiece is at room temperature.

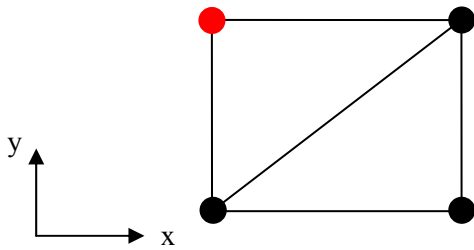


**Figure 3-23.** Illustration of the “upper left node”, here marked as red, used as the tracer line source referred to in some figures.

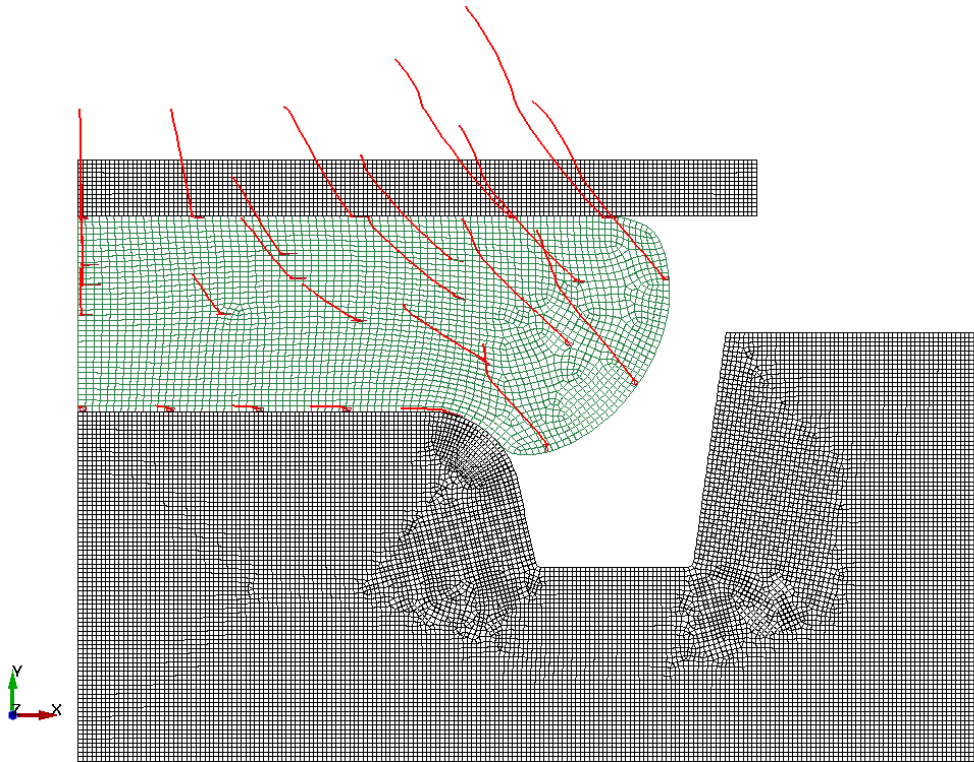


**Figure 3-24.** Tracer lines shown in red for the “upper left node” of the element group used to model each particle during the step 4 forging with inherited stresses and effective plastic strains from step 2 and 3.

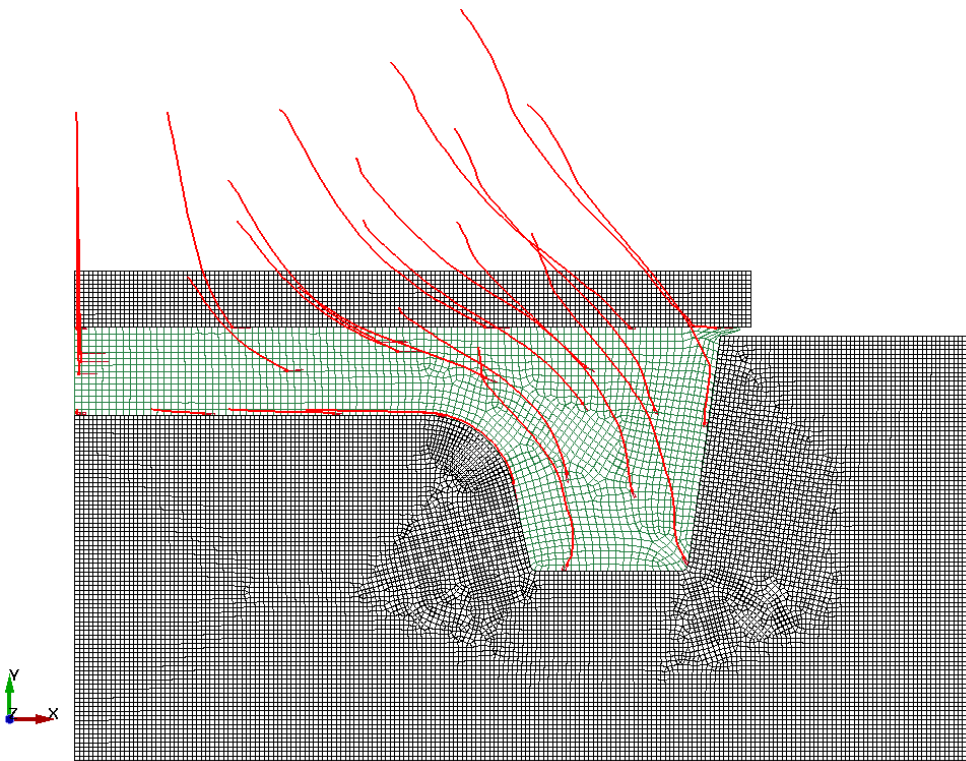


**Figure 3-25.** Tracer lines shown in red for the “upper left node” of the element group used to model each particle, here at the end of step 4, with inherited stresses and effective plastic strains from step 2 and 3.

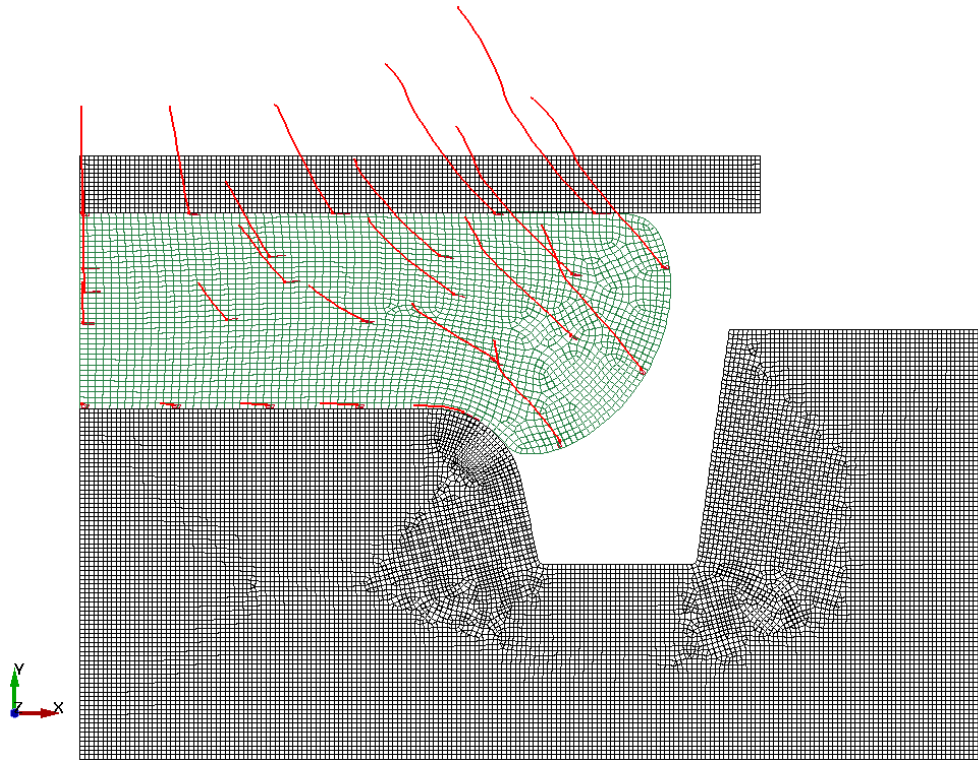


**Figure 3-26.** Tracer lines shown in red for the “upper left node” of the element group used to model each particle during the step 4 forging with inherited stresses and effective plastic strains from step 3 only.

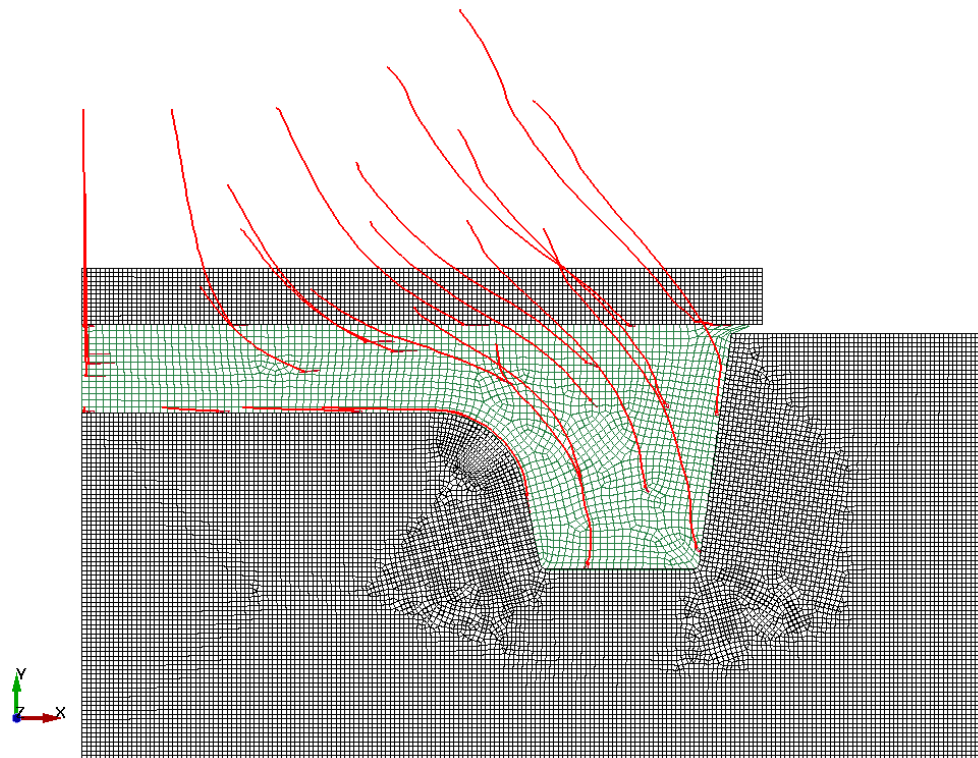


**Figure 3-27.** Tracer lines shown in red for the “upper left node” of the element group used to model each particle, here at the end of step 4, with inherited stresses and effective plastic strains from step 3 only.



**Table 3-4. Initial and final dimensions of postulated “particles” before and after each manufacturing step. In the manufacturing step followed by an asterisk (\*) means that the effective plastic strains are inherited from step 2 and 3, not only from step 3.**

Step / defect no.	Initial dimensions		Final dimensions	
	L (mm)	h (mm)	L (mm)	h (mm)
Upsetting / 1 - 5	5,5,5,5,5	5,5,5,5,5	5,5,5,5,5,8	5,4,5,4,5,4,3
Upsetting / 6 - 10	5,5,5,5,5	5,5,5,5,5	7,7,6,5,6,5,6	3,3,3,3,3,5
Upsetting / 11 - 15	5,5,5,5,5	5,5,5,5,5	8,7,5,7,6,5,5	2,2,2,5,3,3,5
Upsetting / 16 - 20	5,5,5,5,5	5,5,5,5,5	7,6,5,6,5,6,5,6	3,3,3,3,3,5
Upsetting / 21 - 25	5,5,5,5,5	5,5,5,5,5	5,5,5,5,5,5,8	4,5,4,5,4,5,4,3
Piercing* / 1 - 5	5,5,5,5,5,8	5,4,5,4,5,4,3	6,7,5,10,7,7,5	3,5,3,2,2,5,2,5
Piercing* / 6 - 10	7,7,6,5,6,5,6	3,3,3,3,3,5	11,5,10,8,5,6,5,5	1,1,5,1,5,2,3
Piercing* / 11 - 15	8,7,5,7,6,5,5	2,2,2,5,3,3,5	12,10,8,6,5	1,1,1,5,2,5,3
Piercing* / 16 - 20	7,6,5,6,5,6,5,6	3,3,3,3,3,5	8,8,8,7,6	2,2,3,3,3
Piercing* / 21 - 25	5,5,5,5,5,5,8	4,5,4,5,4,5,4,3	5,5,5,5,5,5,5,12,5	4,5,4,4,4,2
Piercing / 1 - 5	5,5,5,5,5,8	5,4,5,4,5,4,3	6,7,9,7,5,7,5	3,5,3,2,5,2,5,2,5
Piercing / 6 - 10	7,7,6,5,6,5,6	3,3,3,3,3,5	11,10,8,5,6,5,5	1,1,5,1,5,2,3
Piercing / 11 - 15	8,7,5,7,6,5,5	2,2,2,5,3,3,5	11,5,10,5,8,6,5	1,1,1,5,2,5,3
Piercing / 16 - 20	7,6,5,6,5,6,5,6	3,3,3,3,3,5	8,8,8,7,6	2,2,2,3,3
Piercing / 21 - 25	5,5,5,5,5,5,8	4,5,4,5,4,5,4,3	5,5,6,5,5,6,12,5	4,4,4,4,2
Closed die forging* / 1 - 5	6,7,5,10,7,7,5	3,5,3,2,2,5,2,5	9,14,5,18,5,5,5,17,5	2,1,0,5,2,0,5
Closed die forging* / 6 - 10	11,5,10,8,5,6,5,5	1,1,5,1,5,2,3	22,23,8,5,4,3,5	0,3,0,2,1,2,3,5
Closed die forging* / 11 - 15	12,10,8,6,5	1,1,1,5,2,5,3	24,5,22,8,5,6,5,5	0,2,0,2,1,1,5,2
Closed die forging* / 16 - 20	8,8,8,7,6	2,2,3,3,3	16,14,12,5,8,5,4,5	0,5,0,5,0,5,1,3
Closed die forging* / 21 - 25	5,5,5,5,5,5,5,12,5	4,5,4,4,4,2	8,10,8,5,7,5,17	2,1,5,1,5,2,1
Closed die forging / 1 - 5	6,7,5,10,7,7,5	3,5,3,2,2,5,2,5	8,5,13,19,6,15,5	2,1,0,5,1,5,1
Closed die forging / 6 - 10	11,5,10,8,5,6,5,5	1,1,5,1,5,2,3	21,23,9,4,5,4	0,3,0,2,1,2,3
Closed die forging / 11 - 15	12,10,8,6,5	1,1,1,5,2,5,3	23,21,5,9,6,4,5	0,2,0,3,1,1,5,3
Closed die forging / 16 - 20	8,8,8,7,6	2,2,3,3,3	17,14,12,8,5,4,5	0,5,0,5,0,5,1,5,3
Closed die forging / 21 - 25	5,5,5,5,5,5,5,12,5	4,5,4,4,4,2	8,10,8,5,7,5,17	2,1,5,1,5,2,1

## 4 Discussion and conclusions

Two types of postulated cracks and one type of handling damage have been introduced on the meshed ingot geometry in order to study the effect on the manufactured lid. The aim was to evaluate the risk for remaining traces of these defects in the lid after machining. A drawing of the final lid geometry has been projected on the final lid geometry from the FE simulation. It has been shown that the half-elliptical crack in the lowest position and the two lower circular cracks tend to enter the material of the lid that remains after machining. The postulated handling damage does not enter the material that remains after machining. A circumferential groove as the axi-symmetric 2D-model used here is not likely to be found on the initial workpiece mantle surface, this groove gives a material loss of 13.8 kg or close to 1 %. Generally surface defects on the mid and lower part of the ingot barrel surface are more critical than surface defects on the upper part. Defects that are originating from the mid and lower part of the ingot surface will end up close to the machined corners of the flange on the lid. These positions are critical due to the narrow machining allowance near the flange corners. It means that in the worst case even relative ground defects with depth 10 mm can leave traces on the lid after machining. It should be noted that the thickness of the extended flange in the finished lid will be reduced by 55 mm after the friction stir welding of the lid to the copper tube. This is described in "Tillverkning av kapselkomponenter" (SKBdoc 1175208). 25 postulated particles distributed in the cross section have been used to illustrate the material flow during the specified manufacturing steps. It has been shown that 10 out of the 25 postulated particles end up within the material of the finished machined lid. None of the defects initially located on the workpiece barrel surface, top or bottom surfaces will be present in the machined lid. The material flow is mainly compressive in the height (Y) direction for the central part of the ingot. For the outer part the material flow is dominant in the radial (X) direction. Typically particles number 13 and 14 are moving both in the positive (X) and in the negative (Y) direction, during the material filling of the cavity of the lower tool.

## References

**Hallquist J O, 2006.** LS-DYNA theory manual. Livermore, CA: Livermore Software Technology Corporation.

**Ssemakula H, 2004.** Manufacturing of heavy rings and large copper canisters by plastic deformation. PhD thesis. Royal Institute of Technology, Sweden.

### Unpublished documents

<b>SKBdoc id, version</b>	<b>Title</b>	<b>Issuer, year</b>
1175208, ver 5.0	Tillverkning av kapselkomponenter.	SKB, 2009
1351636, ver 3.0	Process simulation of large copper extrusions.	SKB, 2012
1377246, ver 2.0	Main study - Copper tube extrusion.	SKB, 2013
1392448, ver 1.0	Simulation of forging of lids with different upper tools.	SKB, 2013
1265008, ver 2.0	Control and effects of grain size in extruded copper.	SKB, 2013